Available online at www.sciencedirect.com
ScienceDirect
Medical Engineering & Physics 31 (2009) 364–373
Medical Engineering & Physics
www.elsevier.com/locate/medengphy

A robotic workstation for stroke rehabilitation of the upper extremity using FES

C.T. Freeman [a,*], A.-M. Hughes [b], J.H. Burridge [b], P.H. Chappell [a], P.L. Lewin [a], E. Rogers [a]

[a] School of Electronics and Computer Science, University of Southampton, Southampton SO17 1BJ, UK
[b] School of Health Professions and Rehabilitation Sciences, University of Southampton, Southampton SO17 1BJ, UK

Received 17 October 2007; received in revised form 23 March 2008; accepted 22 May 2008

Abstract

An experimental test facility is developed for use by stroke patients in order to improve sensory-motor function of their upper limb. Subjects are seated at the workstation and their task is to repeatedly follow reaching trajectories that are projected onto a target above their arm. To do this they use voluntary control with the addition of electrical stimulation mediated by advanced control schemes applied to muscles in their impaired shoulder and arm. Full details of the design of the workstation and its periphery systems are given, together with a description of its use during the treatment of stroke patients.

Keywords: Rehabilitation device; Robotics; Electrical stimulation

1. Introduction

Incidence of stroke in the UK is approximately 100,000 new cases each year. Half of all acute stroke patients starting rehabilitation will have a marked impairment of function of one arm, of whom only about 14% will regain useful sensory-motor function [1,2]. It has been argued that arm and hand function is more important than mobility in achieving independence following stroke [2]. The concept of 'learned disuse' is thought to be a significant barrier to recovery of sensory-motor function [3]. Functional electrical stimulation (FES) can provide the experience for the patient of moving and consequently may limit the problem of learned disuse. Previous research has predominantly dealt with its application to paralysed subjects, but it has also been used with some success to improve recovery of upper limb motor control [4]. Recent studies have shown, however, that when stimulation is associated with a voluntary attempt to move the limb, improvement is enhanced [4,5]. FES may also have a direct effect on excitability of the central nervous system. Based on the 'Hebbian Learning Rule' an hypothesis has recently been proposed to explain enhanced motor learning when FES is applied co-incidentally with voluntary drive [6]. Triggering of stimulation through voluntary activity, using sensory information such as the electromyographic (EMG) or myoelectric activity of the same muscle, has been demonstrated [7], but the techniques so far used do not provide the precise control over the applied stimulation necessary to fully exploit this association between the intended movement of the subject and the application of stimulation that helps them to achieve such a movement. To fully test the hypothesis proposed in [6], a controlled environment is therefore needed in which the patient attempts to perform a task using their remaining voluntary action, whilst simultaneously FES is applied using advanced control schemes to aid its completion.

This has motivated the design and construction of an experimental test facility which is capable of presenting upper limb reaching tasks to stroke patients whilst applying FES to assist their movement. A robotic arm is used to provide the necessary controlled environment and also to give the subject additional assistance when necessary. Note that, whilst there exist several robotic devices for the application of robotic

* Corresponding author.
E-mail address: cf@ecs.soton.ac.uk (C.T. Freeman).

1350-4533/$ – see front matter © 2008 IPEM. Published by Elsevier Ltd. All rights reserved.
doi:10.1016/j.medengphy.2008.05.008

therapy to stroke patients through purely mechanical manipulation of their arms (for example the MIT Manus [8] and Gentle/S systems [9]), this form of treatment has hitherto not been combined with the application of FES.

2. Task overview

The task presented to the patient is to track trajectories using their impaired arm whilst in a seated position. In order that the objective is displayed clearly, only trajectories in a fixed horizontal plane are used and the patient's forearm is constrained to move in this plane by a custom-built robot. A data projector mounted above the subject is used to shine an image of the entire trajectory path, as well as a moving spot to indicate the current point that they must follow, onto a target mounted above the subject's hand. A cross-hair on the target clearly shows that point which is intended to follow the moving spot as it progresses along the trajectory path. The experimental test facility is shown in Fig. 1, and the projector is mounted above the subject by means of a telescopic arm support (shown schematically in Fig. 4). A close-up of the target is shown in Fig. 2.

Constant velocity elliptical trajectories are used since they can approximate functional reaching movements similar to those required to perform everyday tasks, but provide a smooth movement for the subject to follow. These trajectories are displayed at three angles, and are shown in Fig. 3 for the case of a right-hand impaired patient. Here the point P_a is the position of the subject's shoulder joint and d is the horizontal distance from it to their elbow. These values are identified in an initial test in which the subject's arm is moved about the workspace in order to determine their range of movement (ROM) (see [10] for details of the identification procedure used). The elbow, when held out to the subject's side, is at point P_c, and point P_b lies halfway between it and point P_a. The angle α has been set at 20°, and the radii, r_1 and r_2, are chosen to vary the applied treatment depending on the particular movement capabilities of each individual subject. One ellipse used has a major axis between points a_1 and a_2, its length dependent on the radii chosen, another has a major axis between points b_1 and b_2, and the last has a major axis between points c_1 and c_2. In each case an eccentricity of $\sqrt{0.96}$ is used. These are termed trajectories A_l^u, B_l^u and C_l^u, respectively, where u and l denote the upper and lower percentage of maximum reach through which the trajectory extends the arm. The workspace of the robotic arm and the area onto which images can be projected enables these trajectories to be used for the vast majority of subjects with the values $l = 50$ and $u = 100$. The time taken, T, to travel once clockwise about the ellipse, starting from point a_1, b_1 or c_1, is used to vary the applied treatment, and takes a value between 5 and 15 s. Each trajectory tracking task is repeated 10 times.

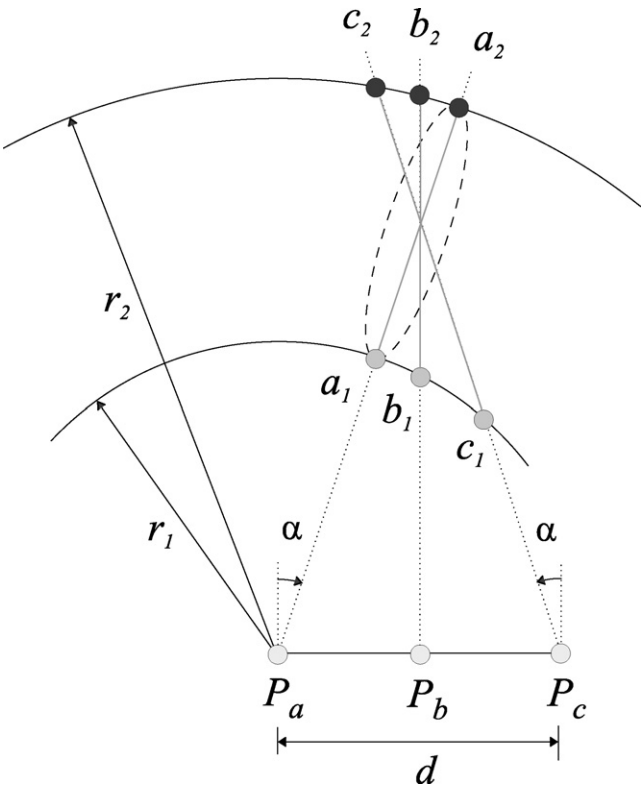

Fig. 3. Reaching trajectories in the horizontal plane for the right-hand case.

Fig. 1. A subject using the workstation whilst FES is applied to their triceps.

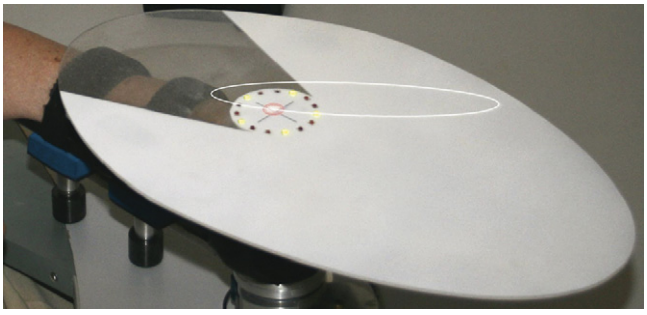

Fig. 2. Close-up of a trajectory projected onto the target.

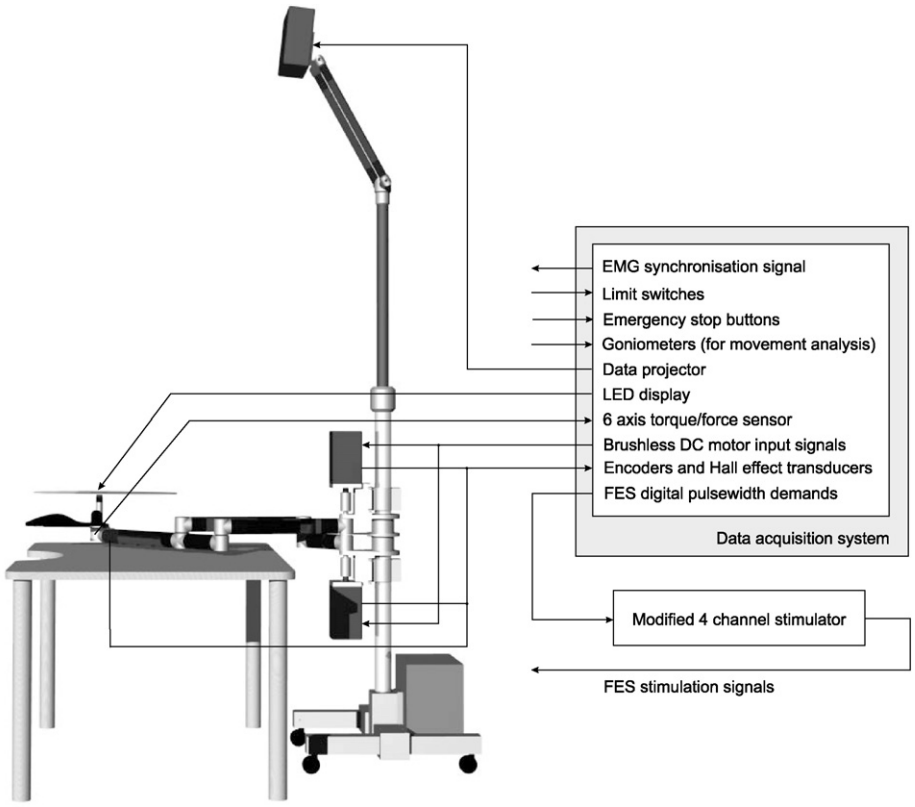

Fig. 4. Schematic representation of the workstation signal requirements.

3. System description

A schematic of the signal requirements of the workstation is given in Fig. 4, and the principal elements of the system are now described.

3.1. Software overview

A schematic of the software and hardware used is shown in Fig. 5. The control scheme has been developed using a graphical simulation environment with extensive control toolboxes enabling rapid prototyping. The real-time model produced is downloaded to a dedicated single-board controller, containing a real-time processor which permits control algorithms to be implemented using a sample frequency of 1.6 kHz. All identification procedures and tracking tasks are initiated by means of a custom written, user-friendly Graphical User Interface (GUI), which uses a real-time interface and set of function libraries to access the control hardware. The GUI communicates with a mathematical software package for access to an extensive data processing library, and also records all experimental test data. A dedicated Visual C++ application which uses the OpenGL graphics application programming interface, together with C libraries for direct access to the control hardware, provides scope to create an engaging environment necessary to promote sustained voluntary effort.

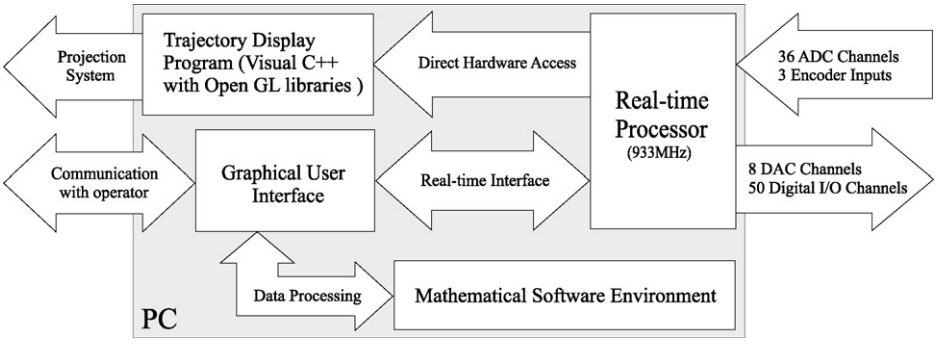

Fig. 5. Software flow diagram.

3.2. Stimulation system

This can deliver 4 channels of stimulation, each comprising a sequence of bi-phasic pulses at 40 Hz. The frequency, amplitude, pulsewidth range and bi-phasic characteristic have been chosen to achieve a smooth muscle contraction (see [11,12] for details). The control hardware uses digital outputs to produce a binary stimulation pulsewidth demand for each channel in the range 0–350 μs with a resolution of 1 μs. Each is then optically isolated and a microcontroller is used to generate a series of 5 V amplitude, 40 Hz pulses with the required pulsewidth for each channel. The amplification stage of a commercial stimulator is then used to produce the desired bi-phasic characteristic and voltage amplitude. The pulsewidth is limited by the control software, the microcontroller circuit, and by components within the modified stimulator. The amplification level used for each channel is set prior to each treatment session by applying a stimulation signal with pulsewidth 350 μs, and slowly increasing the voltage until the maximum comfortable level is reached. See Section 5 for details of the stimulation control system used.

3.3. Robotic arm system

The subject's arm is strapped to the extreme link of a five-bar robotic arm which provides support and constrains it to lie in a horizontal plane. The workspace of the robotic arm covers the 0.87 m × 0.66 m display area onto which the trajectories are projected. The arm is constructed from carbon fibre and aluminium, and is actuated using two DC brushless servomotors, each capable of producing 5.5 N m continuous output torque with a peak torque capability of 14 N m. A 2:1 ratio gearbox is used on each to increase the available torque so that the robot is capable of continuously applying a force of over 13 N (with a peak capability exceeding 33 N) in any direction over the region in which the trajectories described in Section 2 are projected. The motors are driven by modular PWM amplifiers running in torque mode using Hall effect feedback. A 4000-line encoder is mounted on each motor shaft, and an additional 4000-line encoder measures the angle of the link to which the subject's arm is strapped. A six axis force/torque sensor, situated between the penultimate and final links, can measure forces of up to 200 N applied by the subject in the horizontal plane with a resolution of 0.0122 N. See Section 4 for details of the robotic arm control system.

4. Robotic control scheme

A model of the combined human arm and robotic manipulator system is shown in Fig. 6. The robotic arm has a base co-ordinate system with components $\boldsymbol{x}_0$, $\boldsymbol{y}_0$ and $\boldsymbol{z}_0$, and link lengths of $l_1 = 0.45$ m, $l_2 = 0.2$ m and $l_4 = 0.66$ m. The components of the robot input torque, $\boldsymbol{\tau} = [\tau_1 \ \ \tau_2]^{\mathrm{T}}$, are in the directions of ϑ_1 and ϑ_2, respectively, and the subject interacts with the robot by applying a force with components F_x and F_y, in the directions of $\boldsymbol{x}_0$ and $\boldsymbol{y}_0$, respectively, at the point Q which has a z_0 component of l_z in this system. A dynamic model of the robotic arm has been produced using standard identification methods (see [13] for further details).

4.1. Control requirements

The human arm model is composed of two links with length l_u and l_f representing the upper arm and the forearm, respectively. This system has a base co-ordinate frame with components $\boldsymbol{x}_1$, $\boldsymbol{y}_1$ and $\boldsymbol{z}_1$, so that the subject's glenohumeral joint is at position $[0 \ \ 0 \ \ l_u \sin(\gamma)]^{\mathrm{T}}$ in this system. The position components in the constrained z_1 and z_0 directions will now be omitted so that a point, $\boldsymbol{x}$, in the robot co-ordinate system is expressed in the human arm system by a point, $\boldsymbol{x}_a$, such that $\boldsymbol{x} = \boldsymbol{x}_a + [l_x \ \ l_y]^{\mathrm{T}}$ where l_x and l_y represent the $\boldsymbol{x}_0$ and $\boldsymbol{y}_0$ components of the glenohumeral joint position in the robot co-ordinate system. These parameters are found together with l_u, l_f and γ, during the initial ROM test performed with each subject. The variables, ϑ_u and ϑ_f, denote the upper arm and forearm joint angles, respectively, and γ is the elevation angle of the upper arm. A form of

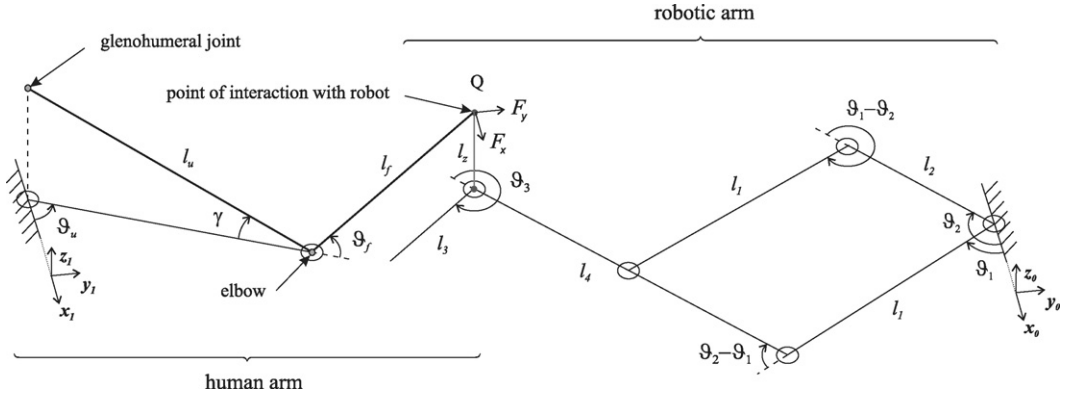

Fig. 6. Geometry of the combined human arm model and five-link robotic arm.

impedance control has been adopted to ensure the safe interaction between robot and human subject [14], and results in the relationship

$$\boldsymbol{h} = \boldsymbol{K}_K\tilde{\boldsymbol{x}} + \boldsymbol{K}_B\dot{\tilde{\boldsymbol{x}}} + \boldsymbol{K}_M\ddot{\tilde{\boldsymbol{x}}} \tag{1}$$

at Q. Here $\boldsymbol{h} = -[F_x \;\; F_y]^{\mathrm{T}}$ denotes the vector of forces applied on the subject by the robot, $\boldsymbol{q} = [\vartheta_1 \;\; \vartheta_2]^{\mathrm{T}}$, $\boldsymbol{J}(\boldsymbol{q})$ is the Jacobian of the system, $\tilde{\boldsymbol{x}} = \hat{\boldsymbol{x}} - \boldsymbol{x}$, $\hat{\boldsymbol{x}}$ is the reference, $\boldsymbol{x} = \boldsymbol{k}(\boldsymbol{q})$ is the direct kinematics equation for the system, $\dot{\boldsymbol{x}} = \boldsymbol{J}(\boldsymbol{q})\dot{\boldsymbol{q}}$, $\ddot{\boldsymbol{x}} = \boldsymbol{J}(\boldsymbol{q})\ddot{\boldsymbol{q}} + \dot{\boldsymbol{J}}(\boldsymbol{q}, \dot{\boldsymbol{q}})\dot{\boldsymbol{q}}$, and $\boldsymbol{K}_K$, $\boldsymbol{K}_B$ and $\boldsymbol{K}_M$ are suitable gain matrices. The acceleration term appearing in (1) is calculated by numerical differentiation. This is performed using a reduced sampling frequency of 64 Hz in order to increase the resolution, and then a 3rd order lowpass Butterworth filter with a 22.5 Hz cut-off frequency is applied to smooth the resulting signal. The necessary actions of the robotic controller are now described.

4.1.1. Case (i): creating a 'natural' feel

During reaching tasks, when not supplying assistance, the robot produces the effect that the subject is moving a point mass through a viscous medium. This therefore approximates the dynamic behaviour experienced during object-moving tasks of the sort commonly encountered in day-to-day life. Such end-effector dynamics will therefore be termed 'natural', and their familiarity helps clarify the control task for the subject, and so promotes the effect of enhanced motor learning when FES is applied co-incidentally with voluntary drive (as hypothesised in [6]). To achieve this, the gain matrices appearing in (1) are set to $\boldsymbol{K}_K = \boldsymbol{0}$, $\boldsymbol{K}_B = K_B\boldsymbol{I}$ and $\boldsymbol{K}_M = K_M\boldsymbol{I}$. The choice of scalar gains $K_B, K_M \geq 0$ is examined in Section 4.2.1 and an additional requirement is that $\hat{\boldsymbol{x}}$ equals a constant value.

4.1.2. Case (ii): tracking control of the subject's arm

The robotic arm must initialise the subject's arm between iterations of the task, and also perform those identification tests needed to produce a dynamic model of the arm (for use in the derivation of stimulation controllers). To move the subject's arm along predefined trajectories, it is necessary to set $\boldsymbol{K}_B = K_B\boldsymbol{I}$, $\boldsymbol{K}_M = K_M\boldsymbol{I}$, $\boldsymbol{K}_K = K_K\boldsymbol{I}$ with $K_K > 0$, and K_B and K_M are then selected to provide the required tracking performance. The choice of the gain values used in practice is examined in Section 4.2.2.

4.1.3. Case (iii): applying assistance

To fully exploit the use of FES to improve on a voluntary attempt at following the target, muscles are selected for stimulation so that torque can be produced about at least one joint throughout the angular range of the movement. At any given time, robotic assistance is supplied to the joint that is not actuated using FES so that the task completion is driven by the electrical stimulation. If both joints are actuated using FES, assistive torque is provided about the one with greatest joint error, and a rate limiter of $\pm 4\mathrm{N\,s}^{-1}$ applied to each in order to ensure a smooth transition exists when assistive torque switches from one joint to the other.

To apply an arbitrary level of assistive torque about each joint independently, the relationship

$$\boldsymbol{h} = \boldsymbol{J}_a^{-T}(\boldsymbol{q}_a)(\boldsymbol{K}_{K_q}\tilde{\boldsymbol{q}}_a - \boldsymbol{K}_{B_q}\dot{\boldsymbol{q}}_a - \boldsymbol{K}_{M_q}\ddot{\boldsymbol{q}}_a) \tag{2}$$

is desirable, with $\boldsymbol{q}_a = [\vartheta_u \;\; \vartheta_f]^{\mathrm{T}}$, $\hat{\boldsymbol{q}}_a = [\hat{\vartheta}_u \;\; \hat{\vartheta}_f]^{\mathrm{T}}$, $\tilde{\boldsymbol{q}}_a = \hat{\boldsymbol{q}}_a - \boldsymbol{q}_a$, and

$$\begin{aligned} &\boldsymbol{K}_{K_q} = \mathrm{diag}\{K_{K_1}, K_{K_2}\}, \qquad \boldsymbol{K}_{B_q} = \mathrm{diag}\{K_{B_1}, K_{B_2}\}, \\ &\boldsymbol{K}_{M_q} = \mathrm{diag}\{K_{M_1}, K_{M_2}\} \end{aligned} \tag{3}$$

where $K_{K_1}, K_{K_2}, K_{B_1}, K_{B_2}, K_{M_1}, K_{M_2} \geq 0$. Through selection of these gains, arbitrary second order dynamics may be independently imposed about both the elbow and shoulder joints. In particular, when only an assistive torque about the shoulder is required, $\hat{\boldsymbol{x}}_a$ is the point of intersection of a line extending along the forearm and the trajectory, as shown in Fig. 7(a), in which $\boldsymbol{x}_a^*(t) = \boldsymbol{k}_a(\boldsymbol{q}_a^*(t))$ where the desired joint trajectory is given by $\boldsymbol{q}_a^*(t) = [\vartheta_u^*(t) \;\; \vartheta_f^*(t)]^{\mathrm{T}}$. When instead an assistive torque about the elbow is desired, $\hat{\boldsymbol{x}}_a$ is located at the intersection of the trajectory with a line through the shoulder and $\boldsymbol{x}_a$, as shown in Fig. 7(b). Note

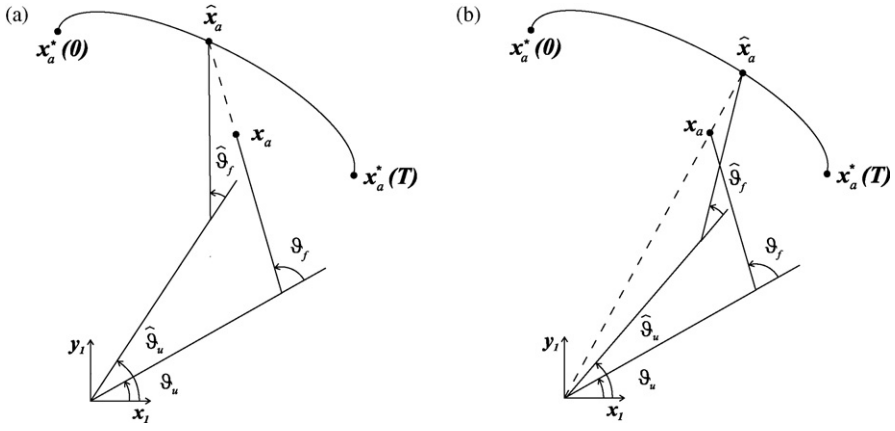

Fig. 7. Values of $\hat{\boldsymbol{x}}_a$ to return arm to the trajectory path for assistive torque applied about (a) the shoulder, and (b) the elbow.

Table 1
Mean acceleration and velocity and associated mean dynamics error for 3 parameter sets (S.D. in brackets)

Parameter set	K_B (N/ms^{-1})	K_M (N/ms^{-2})	Mean velocity (ms^{-1})	Mean acceleration (ms^{-2})	Mean dynamics error (N) [%]
1	20	0.8	0.053 (0.010)	0.367 (0.122)	0.120 (0.026) [11.9 (2.5)]
2	30	1.2	0.083 (0.015)	0.478 (0.150)	0.191 (0.069) [5.0 (1.7)]
3	40	1.6	0.193 (0.041)	1.047 (0.337)	0.430 (0.137) [5.9 (2.0)]

that in both of these cases $\hat{\boldsymbol{x}}_a$ is purely used for computation of the supportive torque given by the robot. It may not be immediately obvious that a static torque applied in the directions $\hat{\boldsymbol{x}}_a - \boldsymbol{x}_a$ shown in Fig. 7(a) and (b) produces only torque about the shoulder and elbow, respectively, but this is easily verified by right-multiplying the transposed system Jacobian by vectors in the direction of $\hat{\boldsymbol{x}}_a - \boldsymbol{x}_a$ for each case. Suitable choices for these vectors are $[c_{uf}\ s_{uf}]^{\mathrm{T}}$ and $[l_u c_\gamma c_u + l_f c_{uf} \quad l_u c_\gamma s_u + l_f s_{uf}]^{\mathrm{T}}$, respectively, where $c_\gamma = \cos(\gamma)$, $c_u = \cos(\vartheta_u)$, $c_{uf} = \cos(\vartheta_u + \vartheta_f)$ and similarly for the case of $\sin(\cdot)$.

The resulting control scheme can deliver the required arbitrary level of assistive torque about the glenohumeral joint for tracking of $\hat{\vartheta}_u$ through choice of K_{K_1}, K_{B_1} and K_{M_1}, and can also simultaneously deliver an arbitrary level of assistive torque about the elbow for tracking of $\hat{\vartheta}_f$ through suitable choice of K_{K_2}, K_{B_2} and K_{M_2}. Suitable gain values, K_{K_1}, K_{K_2}, K_{B_1}, K_{B_2}, K_{M_1} and K_{M_2} for applying the assistance in practice are examined in Section 4.2.3. A more formal derivation of $\hat{\boldsymbol{x}}_a$, together with the necessary values of $\boldsymbol{K}_K$, $\boldsymbol{K}_B$ and $\boldsymbol{K}_M$ appearing in (1), is provided in [15].

4.2. Controller validation

Experimental results from a study in which tests were conducted on 18 unimpaired subjects (mean age 57 years, 10 months; standard deviation (S.D.) 5 years, 4 months) are now presented to confirm that the robotic arm can perform the required actions.

4.2.1. Case (i): creating a 'natural' feel

Each subject in the preliminary study was instructed to track trajectories A^i_{55}, B^i_{55} and C^i_{55} three times, with values of $i = \{75, 85, 95\}$, and $T = \{5, 10, 15\}$ s. In order to add variety to the tracking tasks, the tests were conducted for each of the three parameter sets shown in the first 3 columns of Table 1. The Root Mean Square (RMS) of the difference between the desired and actual force experienced by the subject was recorded for each experiment, and the mean value over all experiments is given in the right-hand column of Table 1. This has a small magnitude for each parameter set, and also comprises a small percentage of the total force supplied by the robot (shown in square brackets). The mean and

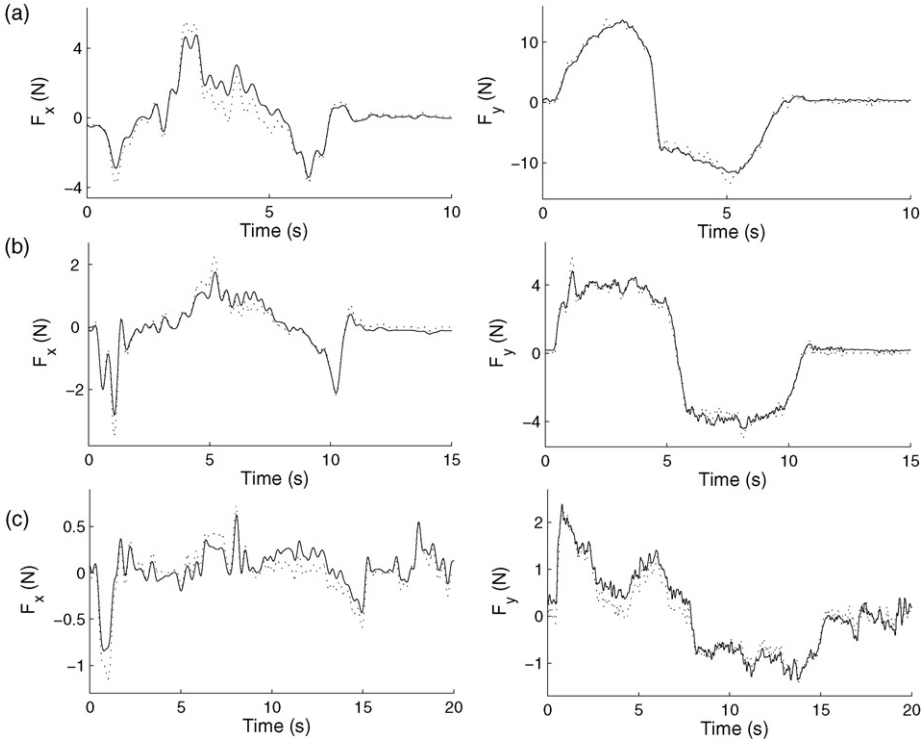

Fig. 8. Experimental (solid line) and desired (dotted line) force during free movement for parameter sets (a) 1, (b) 2, and (c) 3.

standard deviation of the velocity and acceleration also provide information relating to the kinematic region in which the control scheme is required to act. To illustrate the high level of controller performance which can be achieved, representative results for the experimental and desired dynamics are shown in Fig. 8(a)–(c) which correspond to trajectories A_{55}^{75}, B_{55}^{85} and C_{55}^{95}, respectively. The oscillations in the applied force are purely due to the subject constantly making small corrective movements in order to track the trajectory.

4.2.2. Case (ii): tracking control of human arm

Each subject was presented with A_{55}^{95}, B_{55}^{95} and C_{55}^{95} trajectories, each using $T = \{5, 10, 15\}$ s. The tracking control scheme was applied using $K_M = 1.35\text{N/ms}^{-2}$, $K_K = 325\,\text{N/m}$ and $K_B = 55\,\text{N/ms}^{-1}$. To determine the tracking capabilities under different conditions, each tracking task was repeated three times. During the first repetition, the subjects provided no voluntary resistance to the movement, during the second they were instructed to provide a 'low' level of resistance, and during the third they were asked to provide a 'high' level of resistance to the movement. Fig. 9(a) shows an example of the tracking x and y components achieved in each of the three cases for the 15 s C_{55}^{95} trajectory, and Fig. 9(b) shows the corresponding force components applied at the robotic end-effector. In the case of no voluntary resistance to the movement, the mean and standard deviation (S.D.) of the RMS tracking error recorded for subjects over all trajectories of 15 s duration are 7.91 mm and 3.02 mm, respectively. For the case of the 10 s trajectories these are 9.32 mm (S.D. 3.34 mm), and for the case of the 5 s trajectories these are 12.08 mm (S.D. 3.92 mm). The results for the case of 'low' and 'high' levels of resistance show greater variation due to the subjective nature of the instruction given to the patient, but confirm that a significant force can be applied to assist the performance of tracking tasks in a stable manner.

4.2.3. Case (iii): applying assistance

The robotic control scheme described in Section 4.1.3 has been tested using the case in which electrical stimulation is applied to the triceps in order to provide a torque about the elbow. The assistive control scheme is then required to provide torque about the shoulder if insufficient voluntary action means that the shoulder angle error exceeds the elbow angle error. In order to rigorously test the robotic assistance, tests were conducted in which the subjects were instructed to exert no voluntary effort whatsoever, this being verified using Electromyographic (EMG) recordings from unstimulated muscles. The first half of trajectories A_{55}^{95} and C_{55}^{95} have been used since the triceps was assumed to produce torque only in the direction of elbow extension. In this case, the desired relationship given by (2) means that robotic assistance is required to produce a torque about the subject's shoulder of

$$K_{K_1}\tilde{\vartheta}_u - K_{B_1}\dot{\vartheta}_u - K_{M_1}\ddot{\vartheta}_u \tag{4}$$

for the tracking of $\hat{\vartheta}_u$ by ϑ_u, and a torque about the subject's elbow of

$$-K_{B_2}\dot{\vartheta}_f - K_{M_2}\ddot{\vartheta}_f \tag{5}$$

to result in dynamics about the elbow joint that feel natural to the subject. The efficacy of the assistance applied is examined in Fig. 10 for the A_{55}^{95} trajectory, in which representative results are given for both the tracking of $\hat{\vartheta}_u$, as well as the dynamics about the elbow. Fig. 10(a) relates to a 7.5 s trajectory, and Fig. 10(b) to a 5 s trajec-

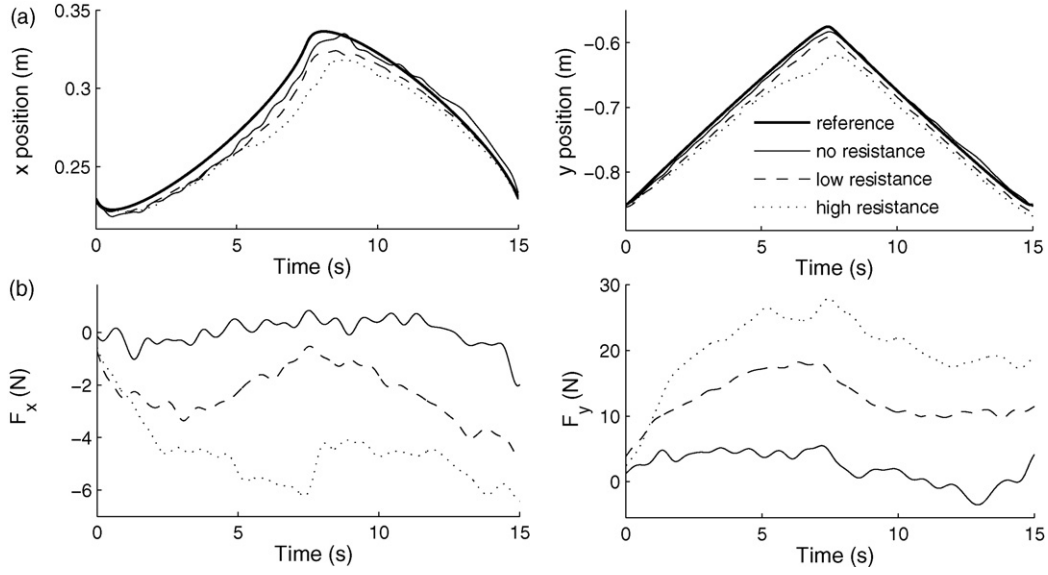

Fig. 9. C_{55}^{95} 15 s reference (a) experimental tracking, and (b) applied force results in x and y directions for the case of a subject applying 3 levels of resistance to movement.

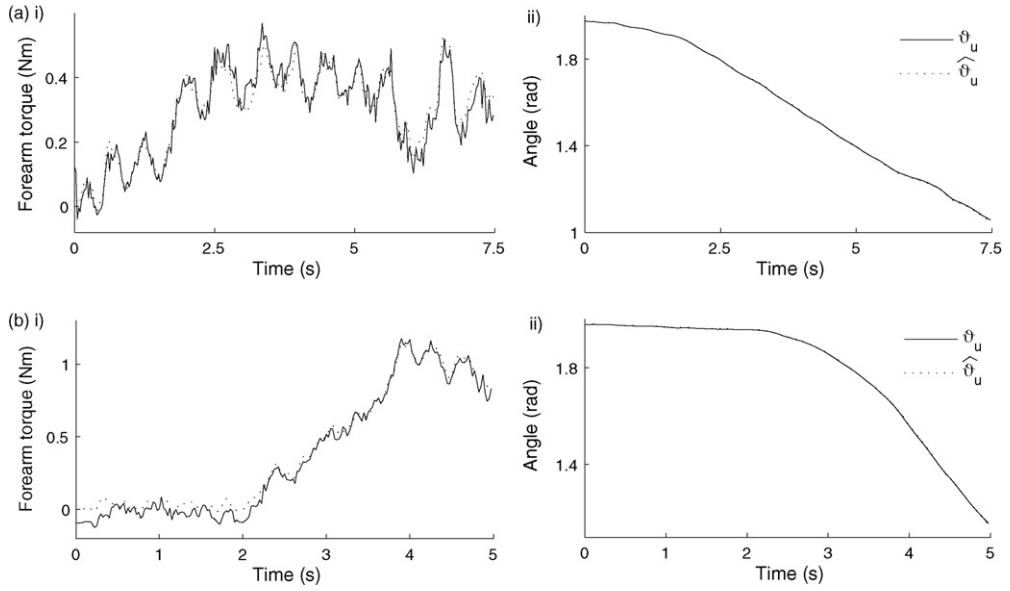

Fig. 10. Assistance verification for (a) 5 s and (b) 7.5 s A_{55}^{95} demands: (i) dynamics about forearm showing reference (solid line) and experimental torque (dotted line), and (ii) tracking of $\hat{\vartheta}_u$ by ϑ_u.

Table 2
Mean subject RMS error for assistance (S.D. in brackets)

Length (s)	Mean $\hat{\vartheta}_u$ tracking error (rad)		Mean forearm dynamics error (N m)	
	A_{55}^{95}	C_{55}^{95}	A_{55}^{95}	C_{55}^{95}
7.5	0.0303 (0.0097)	0.0298 (0.0107)	0.1209 (0.0293)	0.1341 (0.0286)
5	0.0233 (0.0031)	0.0261 (0.0030)	0.1206 (0.0341)	0.1303 (0.0346)

tory. The gains chosen in this case are $K_{K_1} = 22.5\,\mathrm{N\,m/rad}$, $K_{B_1} = 3.6\,\mathrm{N\,m/rad\,s^{-1}}$, $K_{M_1} = 0.09\,\mathrm{N\,m/rad\,s^{-2}}$, $K_{B_2} = 2.45\,\mathrm{N\,m/rad\,s^{-1}}$ and $K_{M_2} = 0.05\,\mathrm{N\,m/rad\,s^{-2}}$. In both cases it can be seen that the torque about the elbow is close to that required to make the task appear natural, and that the assistive tracking of $\hat{\vartheta}_u$ performs extremely well. The oscillations in forearm torque seen were intentionally produced by using slightly excessive gains in the stimulation controller for the purpose of more thoroughly testing the response of the robotic arm. The mean and standard deviation of both the RMS tracking error and the RMS forearm dynamics error are given in Table 2 for all trajectories used. Each trajectory was repeated 10 times with each subject, and the results confirm the robotic controller's ability to simultaneously assist movement whilst also applying dynamics that feel natural to the subject.

5. Stimulation control scheme

The dynamic human arm model is given by

$$\boldsymbol{B}_a(\boldsymbol{q}_a)\ddot{\boldsymbol{q}}_a + \boldsymbol{C}_a(\boldsymbol{q}_a, \dot{\boldsymbol{q}}_a)\dot{\boldsymbol{q}}_a + \boldsymbol{F}_a(\boldsymbol{q}_a, \dot{\boldsymbol{q}}_a) = \boldsymbol{\tau}_a + \boldsymbol{J}_a^T(\boldsymbol{q}_a)\boldsymbol{h} \tag{6}$$

where the general form of the function $\boldsymbol{F}_a(\boldsymbol{q}_a, \dot{\boldsymbol{q}}_a)$ has been assumed on the basis of its performance in experimental tests, and $\boldsymbol{\tau}_a = \boldsymbol{F}(\boldsymbol{u}, \boldsymbol{q}_a, \dot{\boldsymbol{q}}_a)$ represents the torque generated by stimulated muscles. The stimulation control scheme must provide the stimulation input vector, $\boldsymbol{u}(t)$, each element of which specifies the pulsewidth of the FES applied to a single stimulated muscle at time t, in order that $\boldsymbol{q}_a(t)$ tracks $\boldsymbol{q}_a^*(t)$, when applied in combination with suitably chosen assistance provided by the robot. The approach taken is shown in Fig. 11,

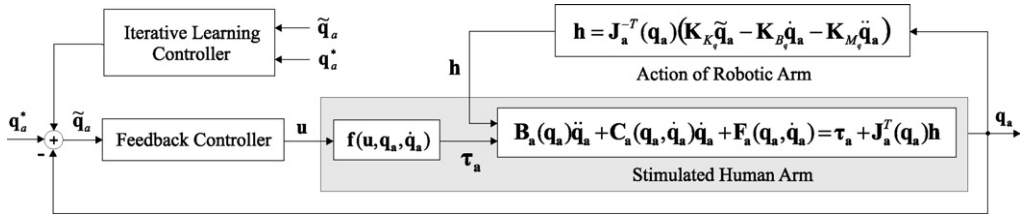

Fig. 11. Control scheme for multi-channel stimulation.

Table 3
Mean of subject RMS error for FES tracking (S.D. in brackets)

Length (s)	Mean tracking error (m)	
	A_{55}^{95}	C_{55}^{95}
7.5	0.01041 (0.00367)	0.01222 (0.00757)
5	0.01418 (0.00994)	0.01443 (0.00657)

and consists of a feedback controller in combination with Iterative Learning Control (ILC), a technique that is applicable to systems operating in a cyclical mode. Using information from previous iterations of the task, ILC produces a correction term that is added to the previous input in order to reduce the tracking error over the next iteration (see the survey papers [16,17] for more information). When accurate tracking of the target trajectory is achieved, the stimulation is reduced to promote sustained voluntary effort by the subject. Results from the case that was introduced in Section 4.2.3, in which the triceps is stimulated and the subject contributes no voluntary effort, will be presented to illustrate the level of tracking performance that can be achieved using this form of stimulation controller. Table 3 shows the mean and standard deviation of the RMS tracking error achieved by the 18 subjects tested for all four trajectories used, each being repeated 10 times. The mean tracking error assumes low values in each case, and confirm the efficacy of the dual stimulation and robotic assistance system. Additional details of the feedback and ILC controllers used can be found in [15].

6. Discussion

The purpose of the workstation is to provide a controlled environment in order for FES to be applied to stroke patients co-incidentally with their remaining voluntary intention. However, for a given trajectory tracking task, there are a wide variety of muscles that may be stimulated, an extensive range of FES control approaches that can be used, and many possible protocols which can be implemented to govern the level of robotic assistance and stimulation applied in order to attempt to maximise the voluntary effort supplied by the patient.

A general overview of the system has been presented in this paper, and the requirements and capabilities that are necessary during all forms of treatment conducted using the workstation have been highlighted. The purpose of the experimental results presented for the robot arm and stimulation controllers has been to illustrate their ability to provide functionality that is applicable and relevant to all cases. This has meant that some details of the experimental results used to validate the system (such as the design of the stimulation controller used in Sections 4.2.3 and 5, and details of the tests used to create a biomechanical models of the arm that is required in its derivation) have not been included, in order to maintain focus on the wider purpose of the system and the breadth of treatment that may be applied using it (although references have instead been provided to this work).

7. Conclusions and future work

The design and functionality of a robotic workstation for use by stroke patients to increase sensory-motor control of their impaired upper limb, has been described. Details of the individual components of the system have been presented, along with experimental results in order to confirm their satisfactory performance. Clinical trials have recently finished involving 5 stroke patients, each receiving courses of treatment comprising up to 25 visits of 1 h duration. Stimulation has only been applied to a single muscle, but its application will shortly be extended to further muscles.

Acknowledgement

This work is supported by the Engineering and Physical Sciences Research Council (EPSRC), grant no. EP/C51873X/1.

Conflict of interest

There are no conflicts of interest.

References

[1] Royal College of Physicians. Stroke: towards better management. London: Royal College of Physicians; 1989.
[2] Wade DT, Langton-Hawer R, Wood VA, Skilbeck CE, Ismail HM. The hemiplegic arm after stroke: measurement and recovery. Journal of Neurology, Neurosurgery, and Psychiatry 1983;46(4):521–4.
[3] Castro-Alamancos M, Garcia-Segura L, Borrell J. Transfer of function to a specific area of the cortex after induced recovery from brain damage. European Journal of Neuroscience 1992;4(9):853–63.
[4] Burridge JH, Ladouceur M. Clinical and therapeutic applications of neuromuscular stimulation: A review of current use and speculation into future developments. Neuromodulation 2001;4(4):147–54.
[5] Sinkjaer T, Popovic D. Peripheral nerve stimulation in neurological rehabilitation. In: In 3rd world congress in neurological rehabilitation. 2002.
[6] Rushton DN. Functional electrical stimulation and rehabilitation—an hypothesis. Medical Engineering and Physics 2003;25(1):75–8.
[7] Thorsen R, Spadone R, Ferrarin M. A pilot study of myoelectrically controlled FES of upper extremity. IEEE Transactions on Neural Systems and Rehabilitation Engineering 2001;9(June (2)):161–8.
[8] Krebs HI, Hogan N, Aisen ML, Volpe BT. Robot-aided neurorehabilitation. IEEE Transactions on Rehabilitation Engineering 1998;6:75–87.
[9] Loureiro R, Amirabdollahian F, Topping M, Driessen B, Harwin W. Upper limb mediated stroke therapy—gentle/s approach. Journal of Autonomous Robots 2004;15(1):35–51.
[10] Freeman CT, Hughes AM, Burridge JH, Chappell PH, Lewin PL, Rogers E. An experimental facility using functional electrical stimulation for stroke rehabilitation of the upper limb. In: Proceedings of 10th IEEE International Conference on Rehabilitation Robotics. 2007. p. 393–400.
[11] De Kroon JR, IJzerman MJ, Chae JJ, Lankhorst GJ, Zilvold G. Relation between stimulation characteristics and clinical outcome in studies using electrical stimulation to improve motor control of

the upper extremity in stroke. Journal of Rehabilitation Medicine 2005;37(2):65–74.

[12] McNeal D, Baker LL, McCaffrey S, Lopez J. Subject preference for pulse frequency with cutaneous stimulation of the quadriceps. In: Proceedings of the 9th Annual Conference of the Rehabilitation Engineering Society of North America. 1986. p. 273–5.

[13] Freeman CT, Hughes AM, Burridge JH, Chappell PH, Lewin PL, Rogers E. An experimental facility for the application of iterative learning control as an intervention aid to stroke rehabilitation. InstMC Measurement + Control 2007;40(February (1)):20–3.

[14] Colgate JE, Hogan N. Robust control of dynamically interacting systems. International Journal of Control 1988;48(1):65–88.

[15] Freeman CT, Hughes AM, Burridge JH, Chappell PH, Lewin PL, Rogers E. Iterative learning control of FES applied to the upper extremity for rehabilitation. Control Engineering Practice; under review.

[16] Bristow DA, Tharayil M, Alleyne AG. A survey of iterative learning control. IEEE Control Systems Magazine 2006;26(3):2039–114.

[17] Ahn H-S, Chen Y, Moore KL. Iterative learning control: Brief survey and categorization. IEEE Transactions on Systems, Man, and Cybernetics Part C: Applications and Reviews 2007;37(6):1099–121.